Int. J. of Applied Mechanics and Engineering, 2022, vol.27, No.2, pp.226-244
DOI: 10.2478/ijame-2022-0030

CHEMICAL REACTION AND MHD FLOW FOR MAGNETIC FIELD EFFECT ON HEAT AND MASS TRANSFER OF FLUID FLOW THROUGH A POROUS MEDIUM ONTO A MOVING VERTICAL PLATE

B. SHANKAR GOUD
Department of Mathematics, JNTUH University College of Engineering Hyderabad,
Kukatpally, Hyderabad, Telangana-500085, INDIA.

MAHANTESH M.NANDEPPANAVAR*
Department of Mathematics, Government College (Autonomous),
Kalaburagi-585105, Karnataka, INDIA
E-mail: nandeppanavarmm@gmail.com

This article discusses the effect of heat and mass transfer in a boundary layer flow in the presence of a magnetic field of an electrically conducting and viscous fluid as it passes through a porous medium containing a heat source and a chemical reaction. By employing similarity variables, the governing equations are changed into nonlinear ordinary differential equations(ODEs). To solve the obtained equations numerically the Keller box method is used. Numerical and graphical representations of the results of different parameter values governing the flow system are given. The non-dimensional distributions of velocity, heat, and concentration are depicted graphically, while the Nusselt number, Sherwood number, and skin friction are determined numerically.

Keywords: MHD, chemical reaction, Keller box method, magnetic field, thermal radiation.

1. Introduction

Chemical engineering, aeronautical plasma flows, electronics, planetary magnetospheres, and stellar magnetospheres are only a few of the areas where MHD free convection flows are used. Physical and engineering issues such as chemical catalytic reactors, geothermal systems, and nuclear waste materials often include natural convective flows due to their importance to thermal insulation, solid matrix heat exchangers, and other practical applications. Instantaneous heat and mass transfer are concepts that are applied to a variety of scientific and engineering problems. In everyday scenarios, formation and crop damage caused by freezing and pollution of the environment, and distribution of temperature illustrate both the heat and mass transfer concept. Practical scenarios also describe the applications of convective heat and mass transfer.

Preservation and combustion systems of nuclear reactors, and solar collectors, in addition to metallurgy and many engineering branches, are controlled by both the effect of buoyancy forces caused by heat and mass diffusion in the presence of a chemical reaction. Chamkha and Khaled [1] studied the problem of coupled heat and mass transfer through MHD free convection flow with internal heat generation or absorption. Ali [2] investigated the influence of suction/injection on the stretched surface power-law thermal boundary. Kandasamy *et al.* [3] inspected heat and mass transfer under a chemical reaction with a heat source. Raptis and Perdikis [4] analyzed a viscous flow over a nonlinear stretching sheet with magnetic and chemical reaction.

Azhar Ali *et al.* [5] used the homotopy study approach to investigate analytically fluid flow solution over an exponentially extended porous sheet. Molla *et al.* [6] investigated the vertical wavy surface natural convection flow with a uniform surface temperature and heat generation/absorption.

* To whom correspondence should be addressed

Mohamed and Abo-Dahab [7] examined the MHD micropolar fluid flow through a moving vertical porous plate. Ali J. Chamkha [8] investigated a hydromagnetic flow over an accelerating permeable surface affected by the presence of a source/sink. Ibrahim *et al.* [9] studied the effect of radiation and chemical reaction, and Bhasker *et al.* [10] studied the radiation and mass transfer impact on MHD free convection flow. Srinivasacharya and Swamy Reddy [11] considered power-law fluid, some effects of heat and mass transfer on an MHD flow over a vertical plate in a porous medium. Barik and Dash [12] considered an unsteady MHD flow past on inclined porous heated plate with chemical reaction and radiation with viscous dissipation effects.

Chandra Shekar Balla and Kishan Naikoti [13] studied the unsteady MHD convective heat and mass transfer past a vertical plate. Das *et al.* [14] examined the impact of mass transfer on flow past an infinite vertical plate that was started impulsively and maintained a continuous heat flux and chemical reaction. Anuar Ishak [15] examined the radiation effect on MHD boundary layer fluid flow by an exponentially stretching sheet. Magyari and Pantokratoras [16] considered a single note on the impact of thermal radiation on the heat transfer features of different boundary layer flows using the linearized Rosseland approximation. Dash *et al.* [17] considered the natural convective MHD flow of moving viscoelastic fluid through porous media in the presence of a chemical reaction. Hall current effect and chemical reaction on MHD flow in conjunction with an accelerated porous plate that absorbs/generates heat internally were investigated by Kar *et al.* [18]. Orhan and Ahmet Kaya [19] investigated the impacts of viscous dissipating MHD mixed convection fluid flow along with a permeable vertical plate.

Jun Cheng *et al.* [20] presented the homotopy analysis solution of nano boundary layer flows. Elbashbeshy and Bazid [21] examined the effect of suction/injection on heat transfer in a porous medium with internal heat generation. Acharya *et al.* [22] examined the influence of the Hall current and thermal diffusion effect on an unsteady hydromagnetic flow near an infinite vertical porous plate in the presence of a chemical reaction. Makinde [23] examined the convective surface boundary constraints for MHD heat and mass transfer through a moving vertical plate. Gireesh Kumar *et al.* [24] investigated an unsteady MHD flow over an infinite vertical plate. Prasad *et al.* [25] examined mixed convection flow over a non-linear stretching sheet with variable and fluid properties.

The current investigation aimed to explore the impact of a chemical reaction and MHD magnetic field effect on fluid flow through a moving vertical plate through a porous medium. This article refers to Makinde's [23] investigation of the impact of chemical reactions and porous media on fluid flow. By employing similarity transformations, the reduced nonlinear ODEs are obtained, which are then elucidated by utilizing the Keller Box technique. The results were obtained for different values of specified parameters.

2. Formulation of the problem

The fluid discussed here is viscous, and incompressible, and the flow occurs as a result of a vertically moving plate. The x - axis is parallel to the plate, while the y -axis is assumed to be normal to it.

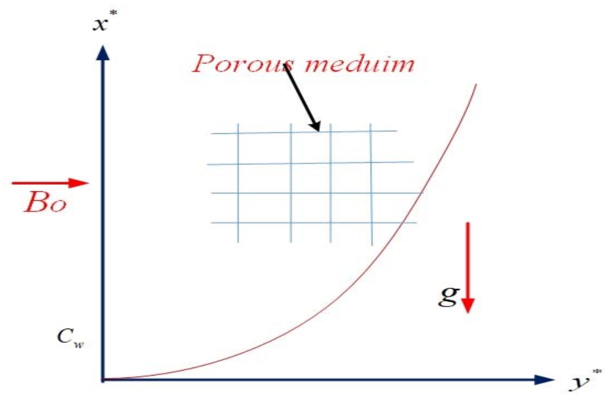

Fig.1. Flow geometry.

Additionally, we, consider a chemical reaction occurring in the presence of a uniform transverse magnetic field of intensity "B_0" in the positive y-axis and also assume the absence of the Hall and electric field effect. The Joule effect is disregarded due to the fluid's limited conductivity. An induced magnetic field is thought to be zero, as is the electric field caused by charge polarization. Due to the low fluid velocity, the energy equation does not define dissipation. Density variance and buoyancy effects have been considered in the equation of momentum. The concentration in the vicinity of the wall is infinitesimally insignificant and therefore ignored. The governing equations for this problem, as approximated by Boussinesq, are as follows:

$$\frac{\partial u}{\partial x}+\frac{\partial v}{\partial y}=0\,, \tag{2.1}$$

$$u\frac{\partial u}{\partial x}+v\frac{\partial v}{\partial y}=\nu\frac{\partial^2 u}{\partial y^2}-\frac{\sigma B_0^2}{\sigma}u-\nu\frac{u}{k_p'}+g\beta\left(T-T_\infty\right)+g\beta^*\left(C-C_\infty\right), \tag{2.2}$$

$$u\frac{\partial T}{\partial x}+v\frac{\partial T}{\partial y}=\alpha\frac{\partial^2 T}{\partial y^2}+S'\left(T-T_\infty\right), \tag{2.3}$$

$$u\frac{\partial C^*}{\partial x}+v\frac{\partial C^*}{\partial y}=D\frac{\partial^2 T}{\partial y^2}+K'\left(C^*-C_\infty^*\right). \tag{2.4}$$

Here, u and v are the velocity elements along the x and y direction.

The appropriate boundary conditions are

$$\left.\begin{array}{l} u(x,0)=U_0\,,\ \ v(x,0)=0,\ \ -k\dfrac{\partial T}{\partial y}(x,0)=h_f\left(T_f-T(x,0)\right),\ \ C_w^*(x,0)=Ax^\lambda+C_\infty^* \\ \\ u(x,\infty)=0, T(x,\infty)=T_\infty, C^*(x,\infty)=C_\infty^* \end{array}\right\}. \tag{2.5}$$

Equation (2.1) is satisfied by the Cauchy-Riemann equations. The velocity components can be defined using the stream function ψ as follows:

$$u=\frac{\partial\psi}{\partial y},\quad v=-\frac{\partial\psi}{\partial x}. \tag{2.6}$$

To translate Eqs (2.2)-(2.5) into a system of ODEs, the subsequent similarity and a non-dimensional variable are used [23]:

$$\eta=\left(\frac{U_0}{\upsilon x}\right)^{\frac{1}{2}}y,\quad \psi=\sqrt{\upsilon x U_o}\,f(\eta),\quad \theta(\eta)=\frac{T-T_\infty}{T_f-T_\infty},\quad C(\eta)=\frac{C^*-C_\infty^*}{C_w^*-C_\infty^*} \tag{2.7}$$

where $f(\eta)$, $\theta(\eta)$ and $C(\eta)$ are the non-dimensional stream function, temperature, and concentration stream functions, respectively.

In Eqs (2.2)-(2.5) can be written as:

$$f''' + \frac{1}{2}ff'' - \left(Ha + \frac{1}{K_p}\right)f' + Gr\theta + GcC = 0\,, \tag{2.8}$$

$$\theta'' + \frac{1}{2}Prf\theta' + ScS\theta = 0\,, \tag{2.9}$$

$$C'' + \frac{1}{2}PrfC' + ScKrC = 0\,. \tag{2.10}$$

The changed boundary conditions are

$$\left.\begin{aligned} &f(0)=0, \quad f'(0)=1, \quad \theta'(0)=-Bi\big(1-\theta(0)\big), \quad C(0)=1 \\ &f'(\infty)=0, \quad \theta(\infty)=0, \quad C(\infty)=0. \end{aligned}\right\} \tag{2.11}$$

Here the prime denotes the differentiation with respect to η.
The dimensionless parameters are:

$$\left.\begin{aligned} &Gr = \frac{g\beta\left(T_f - T_\infty\right)x}{U_0^2}, \quad Gcr = \frac{g\beta^*\left(C_w^* - C_\infty^*\right)x}{U_0^2}, \quad Ha = \frac{\sigma B_0^2 x}{\rho U_0}, \\ &K_p = \frac{k_p' U_0}{\upsilon x}, \quad Kr = \frac{K'x}{U_0}, \quad S = \frac{S'x}{U_0}, \quad \Pr = \frac{\upsilon}{\alpha}, \quad Bi = \frac{h_f}{k}\sqrt{\frac{\upsilon x}{U_0}}, \quad Sc = \frac{\upsilon}{D}. \end{aligned}\right\}$$

Here, all the local parameters Gr, Gc, Ha, Bi, S, Kp, and Kr are the function x in Eqs (2.8) to (2.10). The local skin friction quantity, Nusselt and Sherwood number, and the plate surface temperature are the significant physical quantities. All of these are proportional $f''(0), -\theta'(0)$, and $-C'(0)$ to each other.

3. Solution of the problem

The governing equations (2.8)-(2.10) represent non–linear homogeneous differential equations for which closed-form solutions cannot be obtained. As a result, the (2.8)-(2.10), according to conditions (2.11) are solved numerically by implementing the Keller-box method, which is known as an implicit finite difference method. This method gives the exact outcomes for the boundary layer equations. Since the underlying physical phenomenon is bounded, the numerical range is chosen sufficiently large to satisfy the infinite boundary condition. In the present study, the transverse distance is fixed at 10 (i.e. $\eta \to \infty$). In this method the non-linear ODEs are transformed into simultaneous linear first-ODEs as follows:
So the desired equation can be written as:

$$f' = p\,, \tag{3.12a}$$

$$p' = q\,, \tag{3.12b}$$

$$\theta' = t\,, \tag{3.12c}$$

$$C' = n\,, \tag{3.12d}$$

$$q' + \frac{1}{2} fq - p^2 - Ap + Gr\theta + Gc\,C\,, \tag{3.12e}$$

$$t' + \frac{1}{2} + prft + PrS\theta\,, \tag{3.12f}$$

$$n' + \frac{1}{2} Sc\, f\, n + ScKrC = 0 \tag{3.12g}$$

where $A = M + \dfrac{1}{Kp}$.

The boundary conditions (2.11) change to accommodate the new dependent variable.

$$\left.\begin{aligned} & f = 0, \quad p = 1, \quad t = Bi\big(\theta(0) - 1\big), \quad C = 1 \quad \text{at} \quad \eta \to 0 \\ & p \to 1, \quad \theta \to 0, \quad C \to 0, \quad \text{as} \quad \eta \to \infty. \end{aligned}\right\} \tag{3.13}$$

With the addition of finite-difference approximations for ordinary differential equations (3.12a)-(3.12g), such as average cantered gradients and cantered difference gradients, the Eq.(3.12) changes to:

$$f_j - f_{j-1} = \frac{h_j}{2}\big(p_j + p_{j-1}\big), \tag{3.14a}$$

$$p_j - p_{j-1} = \frac{h_j}{2}\big(q_j + q_{j-1}\big), \tag{3.14b}$$

$$\theta_j - \theta_{j-1} = \frac{h_j}{2}\big(t_j + t_{j-1}\big)\,, \tag{3.14c}$$

$$C_j - C_{j-1} = \frac{h_j}{2}\big(n_j + n_{j-1}\big), \tag{3.14d}$$

$$\begin{aligned} & q_j - q_{j-1} - h_j \left\{ \frac{1}{2}(fq)_{j-\frac{1}{2}} - 2\left(p_{j-\frac{1}{2}}\right)^2 - A\left(\frac{p_j + p_{j-1}}{2}\right) + \right. \\ & \left. + Gr\left(\frac{\theta_j + \theta_{j-1}}{2}\right) + Gc\left(\frac{C_j + C_{j-1}}{2}\right) \right\} = 0\,, \end{aligned} \tag{3.14e}$$

$$t_j - t - h_j\left\{\frac{1}{2}Pr\left(ft\right)_{j-\frac{1}{2}} + PrS\left(\theta\right)_{j-\frac{1}{2}}\right\} = 0\,, \tag{3.14f}$$

$$n_j - n_{j-1} - h_j\left\{\frac{1}{2}Sc\left(fn\right)_{j-\frac{1}{2}} + Kr\left(C\right)_{j-\frac{1}{2}}\right\} = 0\,. \tag{3.14g}$$

Equations (3.14a)-(3.14g) are nonlinear algebraic equations that can be factored in before being linearized. Linearize the system of Eq.(3.14) using Newton's method; now add the following iterations $f_j^{(i+1)} = f_j^{(i)} + \delta f_j^{(i)}$ for all dependent terms and substitute in Eqs (3.14). Calculate the linear tridiagonal equations in the following linear system(simplifying by omitting the superscript):

$$\delta f_j - \delta f_{j-1} - \frac{h_j}{2}\left(\delta p_j + \delta p_{j-1}\right) = \left(r_1\right)_{j-\frac{1}{2}}, \tag{3.15a}$$

$$\delta p_j - \delta p_{j-1} - \frac{h_j}{2}\left(\delta q_j + \delta q_{j-1}\right) = \left(r_2\right)_{j-\frac{1}{2}}, \tag{3.15b}$$

$$\delta\theta_j - \delta\theta_{j-1} - \frac{h_j}{2}\left(\delta t_j + \delta t_{j-1}\right) = \left(r_3\right)_{j-\frac{1}{2}}, \tag{3.15c}$$

$$\delta C_j - \delta C_{j-1} - \frac{h_j}{2}\left(\delta n_j + \delta n_{j-1}\right) = \left(r_4\right)_{j-\frac{1}{2}}, \tag{3.15d}$$

$$\begin{gathered}\delta q_j - \delta q_{j-1} - h_j\left\{\frac{1}{2}f_{j-\frac{1}{2}}\left(\delta q_j + \delta q_{j-1}\right) + \frac{1}{2}q_{j-\frac{1}{2}}\left(\delta f_j + \delta q f_{j-1}\right) - p_{j-\frac{1}{2}}\left(\delta p_j + \delta p_{j-1}\right) - \right.\\ \left. + A\left(\frac{\delta p_j + \delta p_{j-1}}{2}\right) + \frac{Gr}{2}\left(\delta\theta_j + \delta\theta_{j-1}\right) + \frac{Gc}{2}\left(\delta n_j + \delta n_{j-1}\right)\right\} = \left(r_5\right)_{j-\frac{1}{2}},\end{gathered} \tag{3.15e}$$

$$\begin{gathered}\delta t_j - \delta q_{j-1} - Prh_j\left\{\frac{1}{2}f_{j-\frac{1}{2}}\left(\delta n_j + \delta n_{j-1}\right) + \right.\\ \left. + \frac{1}{2}n_{j-\frac{1}{2}}\left(\delta f_j + \delta f_{j-1}\right) + \frac{S}{2}\left(\delta\theta_j + \delta\theta_{j-1}\right)\right\} = \left(r_6\right)_{j-\frac{1}{2}},\end{gathered} \tag{3.15f}$$

$$\begin{gathered}\delta n_j - \delta n_{j-1} - Sch_j\left\{\frac{1}{2}f_{j-\frac{1}{2}}\left(\delta n_j + \delta n_{j-1}\right) + \right.\\ \left. + \frac{1}{2}n_{j-\frac{1}{2}}\left(\delta f_j + \delta f_{j-1}\right) + \frac{Kr}{2}\left(\delta C_j + \delta C_{j-1}\right)\right\} = \left(r_7\right)_{j-\frac{1}{2}}.\end{gathered} \tag{3.15g}$$

Here

$$(r_1)_{j-\frac{1}{2}} = f_{j-1} - f_j + h_j \left(p_{j-\frac{1}{2}} \right), \tag{3.16a}$$

$$(r_2)_{j-\frac{1}{2}} = p_{j-1} - p_j + h_j \left(q_{j-\frac{1}{2}} \right), \tag{3.16b}$$

$$(r_3)_{j-\frac{1}{2}} = \theta_{j-1} - \theta_j + h_j \left(\theta_{j-\frac{1}{2}} \right), \tag{3.16c}$$

$$(r_4)_{j-\frac{1}{2}} = C_{j-1} - C_j + h_j \left(C_{j-\frac{1}{2}} \right), \tag{3.16d}$$

$$\begin{gathered}(r_5)_{j-\frac{1}{2}} = q_{j-1} - q_j - h_j \left\{ \frac{1}{2}(fq)_{j-\frac{1}{2}} - 2\left(p_{j-\frac{1}{2}} \right)^2 - \right. \\ \left. +A\left(\frac{p_j + p_{j-1}}{2} \right) + Gr\left(\theta_{j-\frac{1}{2}} \right) + Gc\left(C_{j-\frac{1}{2}} \right) \right\},\end{gathered} \tag{3.16e}$$

$$(r_6)_{j-\frac{1}{2}} = t_{j-1} - t_j - h_j \left\{ \frac{1}{2} Pr(ft)_{j-\frac{1}{2}} + PrS(\theta)_{j-\frac{1}{2}} \right\}, \tag{3.16f}$$

$$(r_7)_{j-\frac{1}{2}} = n_{j-1} - n_j - h_j \left\{ \frac{1}{2} Sc(fn)_{j-\frac{1}{2}} + Kr(C)_{j-\frac{1}{2}} \right\}. \tag{3.16g}$$

The boundary constraints are

$$\left. \begin{aligned} &\delta f_0 = 0, \quad \delta p_0 = 0, \quad \delta C_0 = 0 \\ &\delta p_j = 0, \quad \delta\theta_j = 0, \quad \delta C_j = 0 \end{aligned} \right\}. \tag{3.17}$$

The difference equations mentioned above can be explained using a block-matrix implementation of the Thomas algorithm. Equations (3.14)-(3.16) can be generated as follows $[Z][\delta]=[\xi]$ in a matrix-vector form.

$$\text{i.e} \begin{bmatrix} [Z_1]\,[C_1] & & & \\ [B_2]\,[Z_2]\,[C_1] & & & \\ & .... & & \\ & & .... & \\ & & [B_{i-1}]\,[Z_{j-2}]\,[C_{i-1}] & \\ & & & [B_j]\,[Z_j] \end{bmatrix} \begin{bmatrix} [\delta_1] \\ [\delta_2] \\ ... \\ .... \\ [\delta_{j-1}] \\ [\delta_j] \end{bmatrix} = \begin{bmatrix} [\xi_1] \\ [\xi_2] \\ ... \\ .... \\ [\xi_{j-1}] \\ [\xi_j] \end{bmatrix}.$$

By taking the step size $\Delta\eta = 0.01$ the effects of improving flow fields over a stretching surface in a nanofluid have been studied for several values of the non-dimensional parameters. The suitable initial guess theories have been selected to determine the method's correctness. With the assistance of boundary conditions, the following initial guesses have been chosen: $f(\eta) = 1 - e^{-\eta}, \theta(\eta) = e^{-\eta}, C(\eta) = e^{-\eta}$.

4. Result in analysis

The numerical outcomes are graphically presented in Figs. 2 to 11, which demonstrate the effect of physical factors incorporated in the flow structure. The Prandtl number(Pr) associated with air was determined to be $Pr = 0.72$. We concentrated on the positive buoyancy factor, viz. the thermal Grashof number $(Gr > 0)$ associated with the cooling plate and the solutal Grashof number $(Gc > 0)$. The impact of the local magnetic field (Ha) and the permeability parameter (Kp) on the velocity profile is depicted in Fig.2. It can be found that increasing Ha eventually leads to a decline in velocity throughout all stages because of the Lorentz force. The effect of Ha the velocity distribution in the absence of permeability is shown in Figure 2, and the findings are consistent with Makinde's work [23]. Additionally, note that when the permeability parameter is present, increasing the magnetic parameter results in a decreased velocity profile.

The influence of the Schmidt number on the velocity profile is revealed in Fig.3 in both the presence and absence of permeability. The Schmidt number denotes the relation between momentum and mass diffusion. In the absence of permeability, the velocity profile marginally decreases as the Schmidt number rises, but significantly falls in the presence of permeability. A related trend in fluid velocity (Fig. 4) has been observed as a result of an improvement in the Bi.

The impact of the local solutal Grashof number on velocity plots is presented in Fig.5 in the presence and absence of permeability. The velocity profile increases as Gc increases. Additionally, the fluid velocity enhances rapidly closes the porous plate and then gradually drops to that of free steam.

Figure 6 portrays the variation of the velocity curves for several values of the thermal Grashof number with and without the existence of a porous medium. The local thermal Grashof number is proportional to the temperature buoyancy force and the viscous force. An enhancement in Gr values leads to a large buoyancy force which increases the fluid flow.

Figure 7 exhibits the impacts of Ha and S on the dimensionless temperature in both the presence and absence of permeability. It shows that the thickness boundary layer enhances as the magnetic field increases. These findings are in agreement with those stated by Makinde [23]. But the thickness of the thermal boundary layer decreases in the occurrence of the source. Again, the existence of a porous medium results in a rise in the thermal boundary layer. However, when both the porous medium and the source are present, the temperature curves reduce as "Ha" increases.

The numerical solutions for the dimensionless temperature field with fixed values of $Gr = Gc = 0.1$, $Ha = 1$, $Pr = 0.72$ for variations in Sc, Bi, S and Kp are shown in Fig.8. In this figure when the source parameter and permeability parameter $(S = 0, Kp = 100)$ are removed, the temperature distribution becomes linear. It is worth noting that the existence of the porous medium $(Kp = 0.5)$ results in an increase in temperature at the Gc points. Regardless of the porous medium. The presence of a source results in a reduction in the temperature curves. By taking into consideration the porous matrix and the source, it was discovered that the thermal boundary layer decreases as Bi enhanced. Additionally, it is established that as Sc rises, the thermal boundary layer expands.

Figure 9 illustrates the influence of Gr and Gc on the temperature profile when the parameters $Ha = 1$, $\Pr = 0.72$, $Kr = 0.5$, $Bi = 0.1$, are fixed. In the presence of a porous matrix, the temperature profile drops down with the thermal buoyancy parameter and alternately accelerates with mass buoyancy.

With fixed values for $Bi = Gr = Gc = 0.1, Kr = 0.5, \Pr = 0.72,$ and $S = 0.2$ Fig.10 depicts the concentration profile for Ha and Sc in the presence and absence of the porous matrix. In the presence of permeability, at all points, the Lorentz force increases the concentrations. The Lorentz force is a resistive force that is generated when a transverse magnetic field is applied to an electrically conducting material. With increasing Sc, the temperature field becomes asymptotic over the boundary layer, which also results in a lowered thermal boundary layer.

Figure 11 demonstrates the influence of the chemical reaction parameter K with fixed values " $\Pr = 0.72,\ Bi = 0.1, Sc = 0.02$ " and " $S = 0.2$ " in the presence/absence of a porous matrix. In the absence of the reaction parameter $(Kr = 0)$, it is observed that porosity increases the temperature field at all stages. When a porous medium is present, the concentration profile changes significantly as the chemical reaction constraint is increased. The concentration curves are asymptotic in nature, which is in agreement with the results of Makinde [23].

To demonstrate the Keller box technique's accuracy, the computed numerical results $\tau(0), \theta'(0)$ and $C'(0)$ are tabulated in Tab.1, by taking different quantities of flow parameters in Tab.1, it is observed that "Sc, Ha, Kp, S, Kr" decreases the skin friction coefficient and vice versa, but that it raises as the buoyancy parameters,"Gr, Gc and Bi" rise. The findings obtained in the absence of "Kp, S, Kc" are similar to Makinde[23]. Increases in Bi, S result in a rise in the Nusselt number, but a reduction in the other parameters. When the value of the parameter Gc, Kr, Sc is increased, a large increase in the Sherwood number is observed, but the table shows the opposite pattern. However, this phenomenon is consistent with Makinde's findings [23].

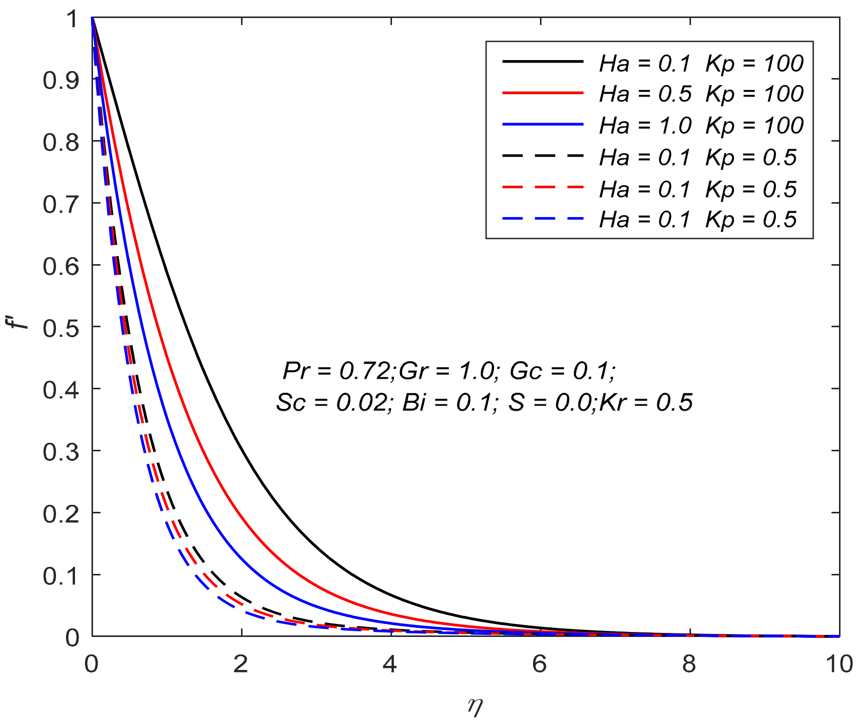

Fig.2. Velocity distribution vs Ha and Kp values.

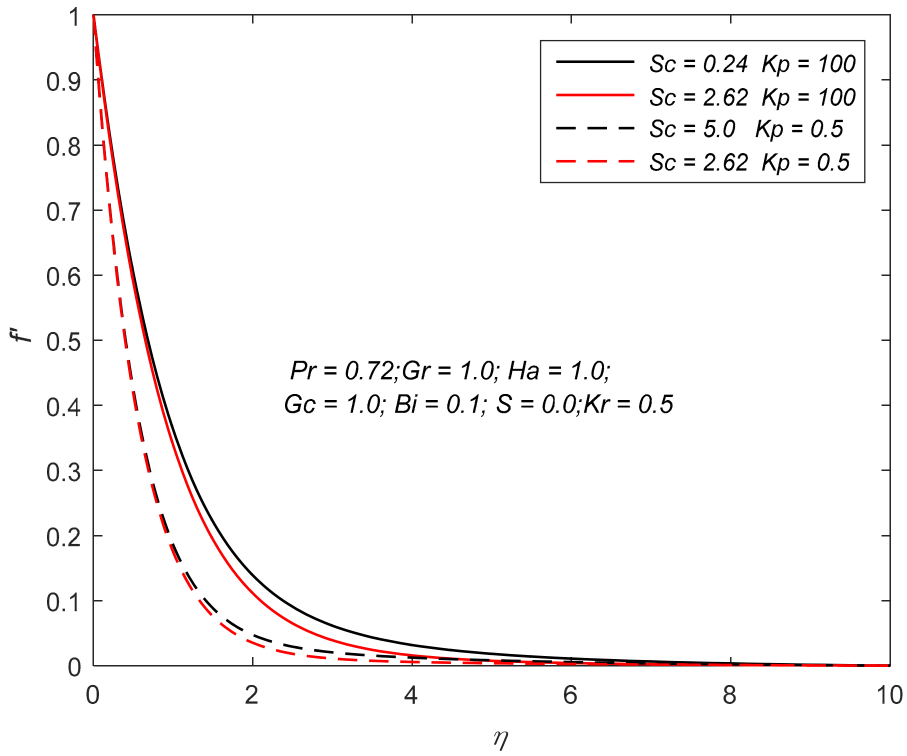

Fig.3. Velocity distribution vs Sc and Kp values.

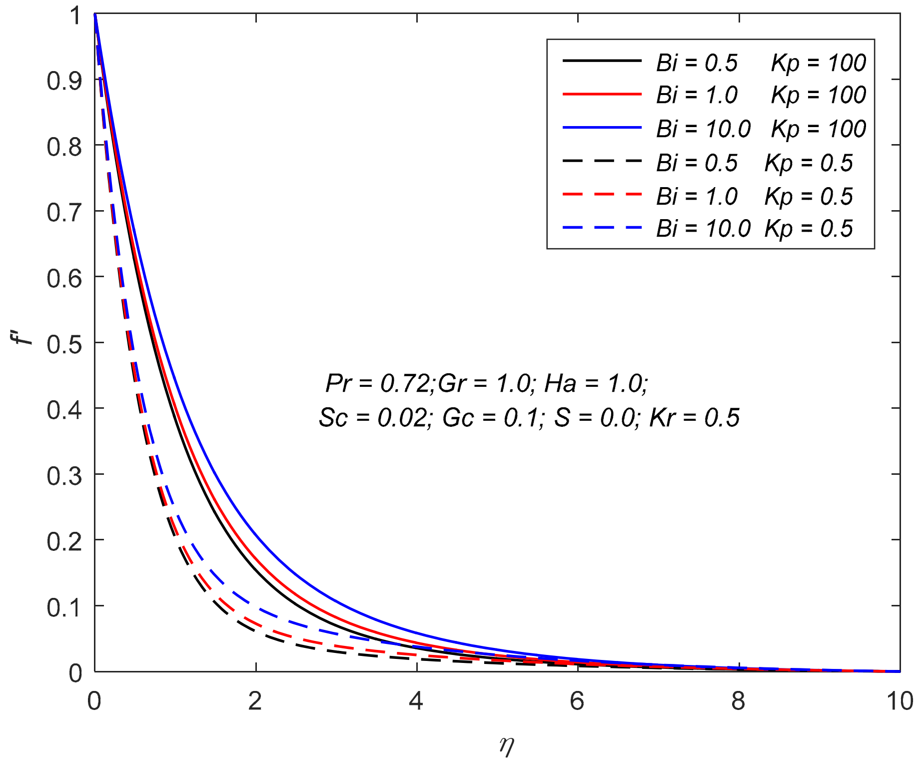

Fig.4. Velocity profile vs Kp and Bi values.

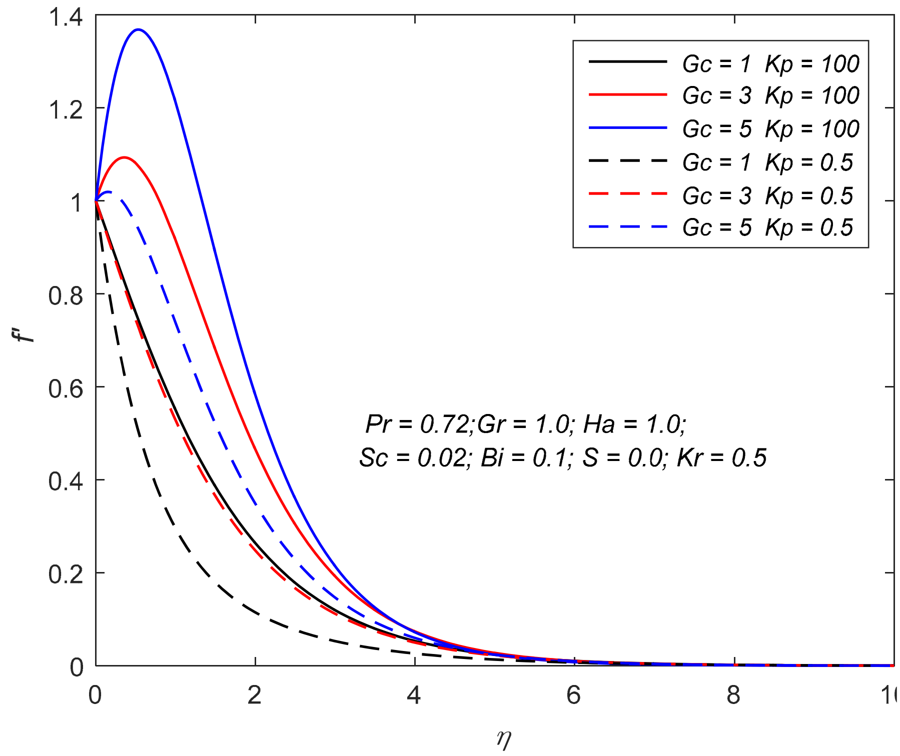

Fig.5. Velocity distribution vs several values of Kp and Gc .

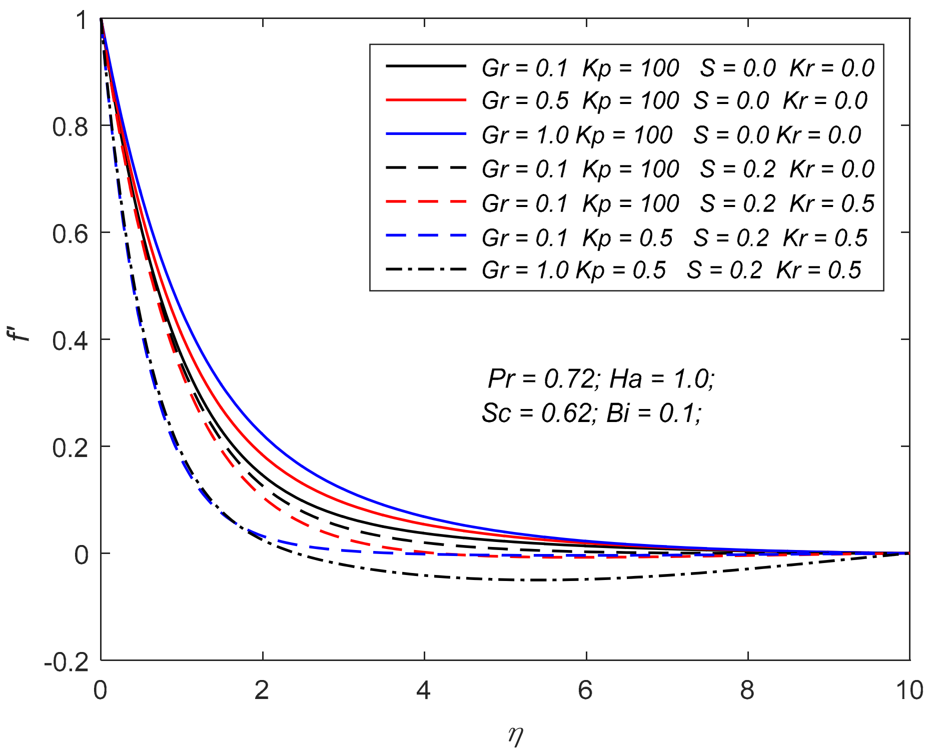

Fig.6. Velocity distribution vs several values of Gr, Kp, S and Kr.

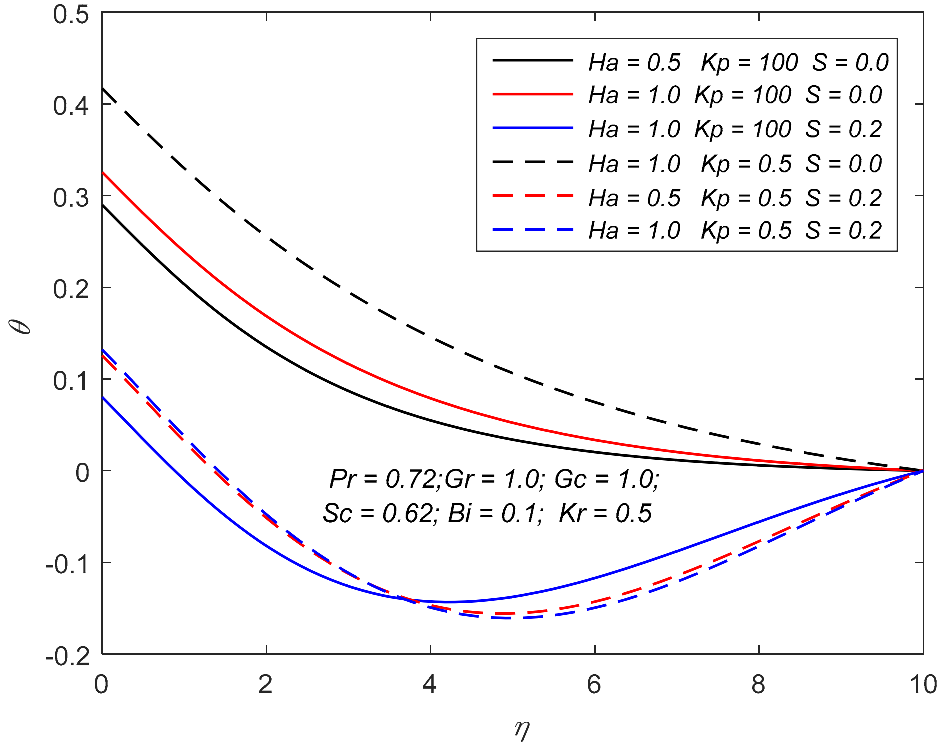

Fig.7.Temperature distribution vs several values of Ha, Kp and S.

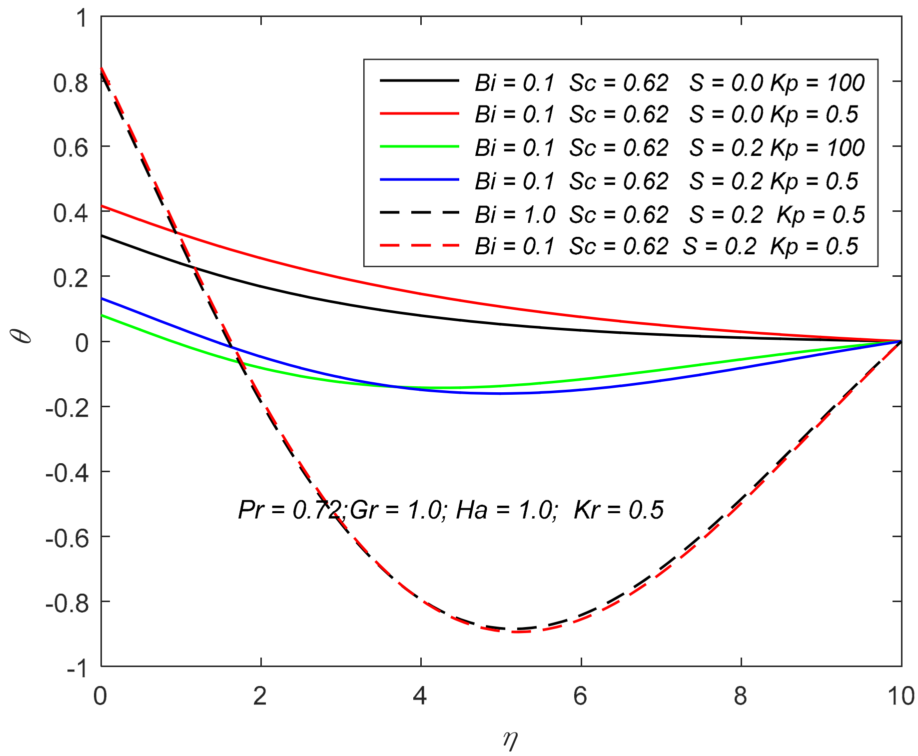

Fig.8.Temperature distribution vs several values of Bi, S, Sc and Kp.

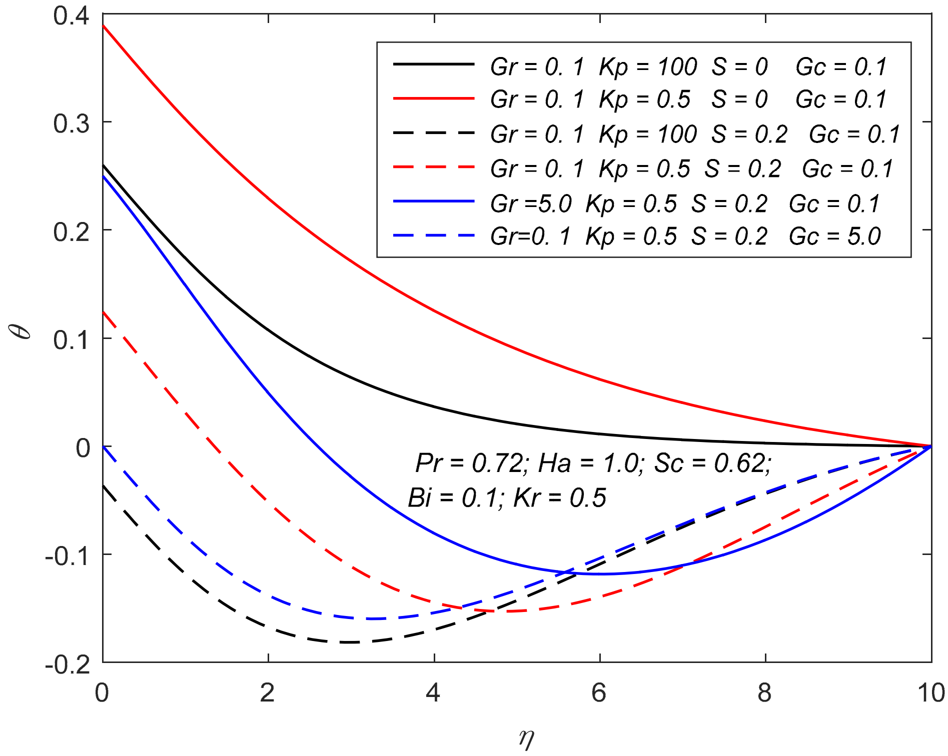

Fig.9. Temperature distribution vs several values of Gr, Gc, S and Kp.

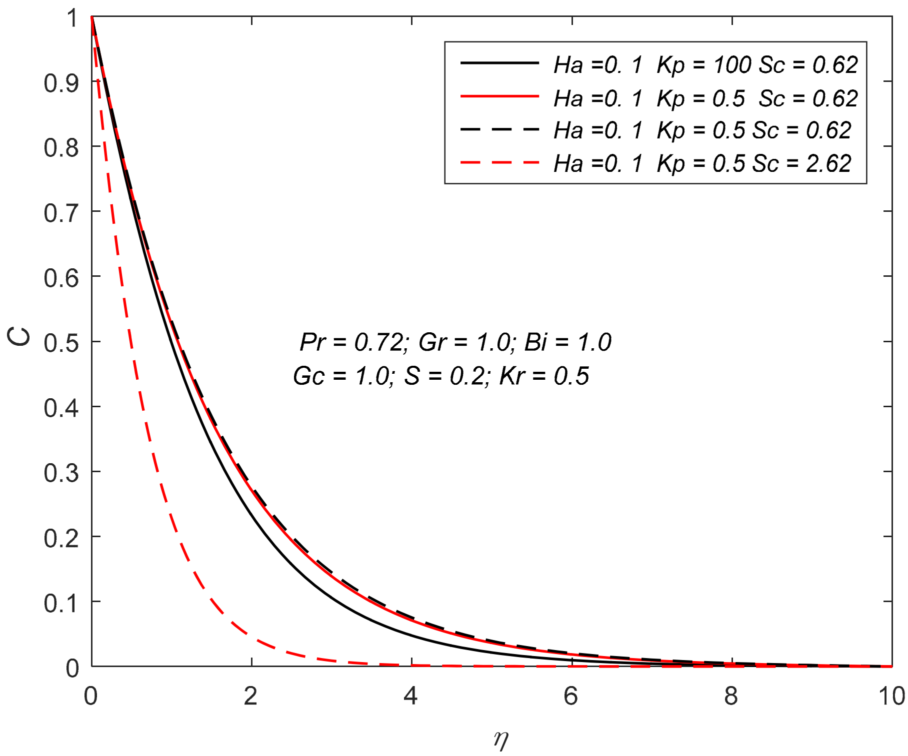

Fig.10. Concentration distribution vs several values of Ha, Sc and Kp.

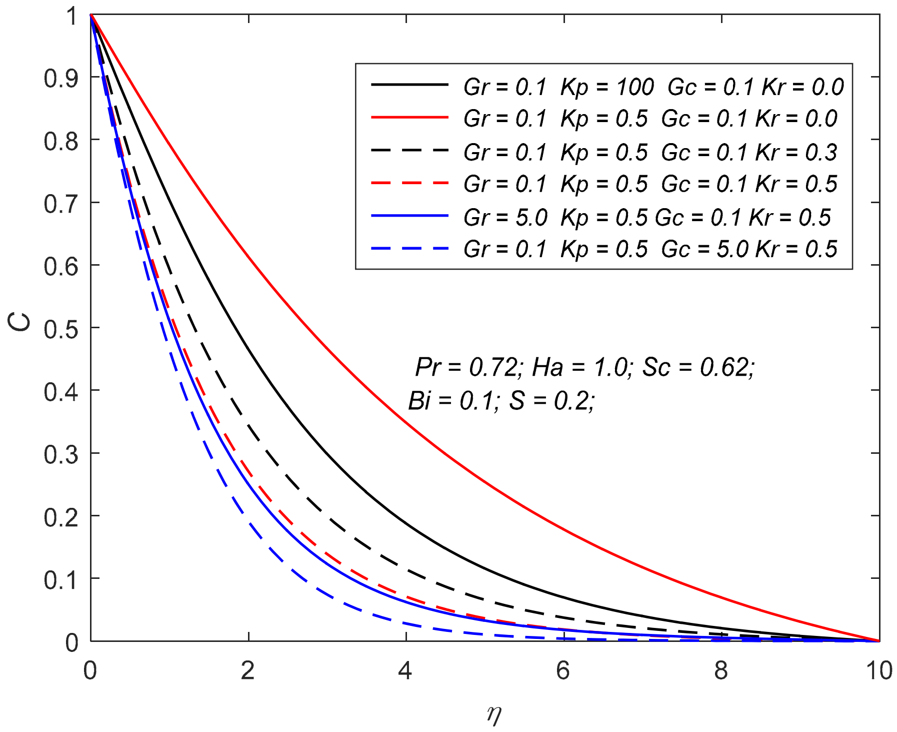

Fig.11. Concentration distribution vs several values of Gr, Gc, Kr and Kp.

Table 1. The values of $\tau(0), \theta'(0)$ and $C'(0)$ for $Pr = 0.72$.

Gr	Gc	Sc	Bi	Ha	Kp	S	Kc	$-\tau(0)$	$-\theta'(0)$	$-C'(0)$
0.1	0.1	0.62	0.1	0.1	100	0	0	0.41811	0.09091	0.41885
							0.1	0.41811	0.09091	0.41885
						0.2		0.49464	0.09091	0.40533
					0.5			1.44767	0.09091	0.34163
				1	100			1.01798	0.09091	0.365
			1	0.1				0.46653	0.5	0.39319
		2.62	0.1					0.52498	0.09091	0.92878
	1	0.62						0.345031	0.09091	0.48099
1	0.1							0.34135	0.09091	0.39463
1					0.5			1.38678	0.09091	0.33954
0.1	1							0.97701	0.09091	0.38231
				1				1.72750	0.09091	0.33042

5. Conclusions

In this work, the Keller box technique was employed to get the numerical results for the MHD free convective flow through a moving vertical plate in the presence of a chemical reaction. The Keller box technique is used to solve the dimensionless governing equations. The velocity temperature and concentration results are obtained and graphically plotted. Tables include the numerical results for $\tau(0), \theta'(0)$ and $C'(0)$. The following are the major findings of this research.

- With an increase in the local magnetic parameter *Ha*, a reduction in velocity has been observed.
- With no porous medium and source parameter, the temperature distribution turns linear.
- The temperature distribution decreases with an increase in the thermal buoyancy parameter.
- An increase of the source parameter decreases the temperature profile, meanwhile, porosity increases the temperature field in all cases.
- With a porous matrix in consideration, the concentration distribution is decreasing.
- An enhancement in the amount of the magnetic field creates an increased temperature and mass thickness of the boundary layer.

Nomenclature

Bi – convective heat transfer parameter
C – dimensionless species concentration
C_p – specific heat at constant pressure $\left(\frac{J}{kg\,K}\right)$
C^* – fluid concentration $\left(kg/m^3\right)$
C_w^* – concentration of the chemical species in the fluid $\left(kg/m^3\right)$
C_∞^* – species concentration at infinity $\left(kg/m^3\right)$
D – mass diffusivity $\left(m^2/s\right)$
g – acceleration due to gravity $\left(kg/s^2\right)$
Gc – solutal Grashof number
Gr – thermal Grashof number
Ha – magnetic parameter
k – thermal conductivity $\left(\frac{W}{m\,K}\right)$
K' – dimensional chemical reaction component
k_p' – coefficient of permeability in a porous medium
Kp – permeability parameter
Kr – chemical reaction parameter
l – the plate source concentration exponent
Pr – Prandtl number
S – source parameter
S' – dimensionless heat generation/ absorption coefficient
Sc – Schmidt number
T – fluid temperature (K)
T_w^* – fluid temperature at the wall (K)
T_∞^* – fluid temperature at infinity (K)

u, v – component of velocity along x, y direction (m/s)

U_0 – plate velocity

α – thermal diffusivity

β – coefficient of thermal expansion (K^{-1})

β^* – expansion of concentration coefficient (m^3/kg)

θ – dimensionless fluid temperature

ν – kinematic viscosity (m^2/s)

ρ – fluid density (kg/m^3)

σ – electrical conductivity of the fluid (S/m)

REFERENCES

[1] Chamkha A.J. and Khaled A.R.A. (2001): *Similarity solutions for hydromagnetic simultaneous heat and mass transfer by natural convection from an inclined plate with internal heat generation or absorption*.– Heat Mass Transfer, vol.37, pp.117-123.

[2] Ali M.E. (1995): *On thermal boundary layer on a power-law stretched surface with suction or injection*.– Int. Journal of Heat and Fluid Flow, vol.16, No.4, pp.280-290.

[3] Kandasamy R, Perisamy K, and Sivagnana Prabhu(2005): *Chemical reaction, heat and mass transfer on MHD flow over a vertical stretching surface with heat source and thermal stratification effects*.– Int. J. Heat Mass Transf., vol.48, pp.4557-4561.

[4] Raptis A and Perdikis C. (2006): *Viscous flow over a nonlinearly stretching sheet in the presence of a chemical reaction and magnetic field*.– Int J Non-Linear Mech., vol. 42, pp.527-529.

[5] Azhar Ali, H. Zaman, M.Z. Abidin andS.I.A. Shah (2015): *Analytic solution for fluid flow over an exponentially stretching porous sheet with surface heat flux in porous medium by means of homotopy analysis method*.– American Journal of Computational Mathematics, vol.5, pp.224-238.

[6] Molla M.M., Hossain M.A. and L.S. Yao. (2004): *Natural convection flow along a vertical wavy surface with uniform surface temperature in presence of heat generation/absorption*.– International Journal of Thermal Sciences, vol.43, No.2, pp.157-163.

[7] Mohamed R. A. and Abo-Dahab S. M. (2009): *Influence of chemical reaction and thermal radiation on the heat and mass transfer in MHD micropolar flow over a vertical moving porous plate in a porous medium with heat generation*.– International Journal of Thermal Sciences, vol.48, pp. 1800-1813.

[8] Ali J. Chamkha (2000): *Thermal radiation and buoyancy effects on hydromagnetic flow over an accelerating permeable surface with heat source or sink*.– International Journal of Engineering Science, vol.38, pp.1699-1712.

[9] Ibrahim F.S., Elaiw A.M. and Bakar A.A. (2008): *Effect of the chemical reaction and radiation absorption on the unsteady MHD free convection flow past a semi infinite vertical permeable moving plate with heat source and suction*.– Commun. Nonlinear Sci.Numer. Simul., vol.13, pp.1056-66.

[10] Bhaskar N.R., Saneetha S., and Ramachandra V.P. (2009): *Radiation and mass transfer effects on MHD free convection flow past an impulsively started isothermal vertical plate with dissipation*.– Therm. Sci. vol.13, No.2, pp.171-181.

[11] Srinivasacharya D. and Swamy Reddy G. (2016): *Chemical reaction and radiation effects on mixed convection heat and mass transfer over a vertical plate in power-law fluid saturated porous medium*.– Journal of the Egyptian Mathematical Society,vol.24, pp.108-115.

[12] Barik R.N and Dash G.C. (2014): *Thermal radiation effect on an unsteady magnetohydrodynamic flow past inclined porous heated plate in the presence of chemical reaction and viscous dissipation.*– Applied Mathematics and Computation, vol.226, pp.423-434.

[13] Chandra Shekar Balla and Kishan Naikoti (2015): *Radiation effects on unsteady MHD convective heat and mass transfer past a vertical plate with chemical reaction and viscous dissipation*.– Alexandria Engineering Journal, vol.54, pp.661-671.

[14] Das U.N., Deka R. and Soundalgekar. V.M. (1994): *Effects of mass transfer on flow past an impulsive started infinite vertical plate with constant heat flux and chemical reaction*.– Forsch.Ingenieurwes, vol.60, pp.284-287.

[15] Anuar Ishak. (2011): *MHD boundary layer flow due to an exponentially stretching sheet with radiation effect*.– SainsMalaysiana, vol.40, No.4, pp.391-395.

[16] Magyari E. and PantokratorasA. (2011): *Note on the effect of thermal radiation in the linearized Rosseland approximation on the heat transfer characteristics of various boundary layer flows*.– Int. Commun. Heat Mass Transfer, vol.38, pp.554-556.

[17] Dash G.C., Rath P.K., N. Mohapatra and Dash P.K. (2009): *Free convective MHD flow through porous media of a rotating visco-elastic fluid past an infinite vertical porous plate with heat and mass transfer in the presence of a chemical reaction.*– AMSE, Model B, vol.78, No.4. pp.21-37.

[18] Kar M., SahooS.N. and DashG.C. (2014): *Effect of Hall current and chemical reaction on MHD flow along an accelerated porous plate with internal heat absorption/generation*.–J. Eng. Phys. Thermo Phys., vol.87, No.3, pp.624-634.

[19] Orhan Aydin and Ahmet Kaya. (2009): *MHD mixed convection of viscous dissipating fluid about a permeable vertical flat plate.*– Applied Mathematical Modelling, vol.33, pp.4086-4096.

[20] Jung Cheng, Shijun Liao, Mohapatra R.N. and Vajravelu K. (2008): *Series solutions of nano boundary layer flows by means of the homotopy analysis method*.– J. Math. Anal. Appl., vol.343, pp.233-245.

[21] ElbashbeshyE.M.A. and Bazid M.A.A.(2004): *Heat transfer in a porous medium over a stretching surface with internal heat generation and suction or injection*.– Appl. Math. Comput.vol.158, pp.799-807.

[22] Acharya M., Dash G.C. and Singh L.P. (1995): *Effect of chemical and thermal diffusion with Hall current on unsteady hydromagnetic flow near an infinite vertical porous plate*.– J. Phys. D Phys., vol.28, pp.2455-2464.

[23] Makinde O.D. (2010): *On MHD heat and mass transfer over a moving vertical plate with a convective surface boundary condition*.– Can. J. Chem. Eng., vol.83, pp.983-990.

[24] Gireesh Kumar J., Satya Narayana P. V. and Ramakrishna S. (2009): *Effects of chemical reaction and mass transfer on MHD unsteady free convection flow past an infinite vertical plate with constant suction and heat sink.*– J. Ultra Sci., vol.21, No.3, pp.12-28.

[25] Prasad K.V., Vajravelu K. and DattiP.S.(2010): *Mixed convection heat transfer over a non-linear stretching surface with variable fluid properties*.– Int. J. Nonlinear Mechanics, vol.45, pp.320-330.

[26] Hari Singh Naik, Shankar Goud B., Suresh P. and Ramana Murthy M.V. (2020): *Suction/injection effects on free convective fluid flow over a moving vertical porous plate with variable time*.– Journal of Critical Reviews, vol.7, No.18, pp.1324-1328.

[27] Shankar Goud B. (2020): *Thermal radiation influences on MHD stagnation point stream over a stretching sheet with slip boundary conditions*.– International Journal of Thermofluid Science and Technology, vol.7, No.2, Article number 070201.

[28] Pramod Kumar P., Shankar Goud.B. and BalaSiddulu Malga.(2020): *Finite element study of Soret number effects on MHD flow of Jeffrey fluid through a vertical permeable moving plate*.– Partial Differential Equations in Applied Mathematics, vol.1, Article number 100005,https://doi.org/10.1016/j.padiff.2020.100005.

[29] Shankar Goud B., Venkata Madhu J. and M.N. Raja Shekar. (2019): *MHD viscous dissipative fluid flows in a channel with a stretching and porous plate with a radiation effect.*– Int. J. Innovative Technol. Explor. Eng., vol.8, No.11, pp.1877-1882.

[30] Thadakamalla Srinivasulu and Shankar Goud B. (2021): *Effect of inclined magnetic field on flow, heat and mass transfer of Williamson nanofluid over a stretching sheet*.– Case Studies in Thermal Engineering, vol.23, Article number 100819, https://doi.org/10.1016/j.csite.2020.100819.

[31] Shankar Goud B., Bindu P., Pudhari Srilatha, and Hari Krishna Y. (2020): *The Joule heating effect on MHD natural convective fluid flow in a permeable medium over a semi-infinite inclined vertical plate in the presence of the chemical reaction*.– IOP Conf. Series: Materials Science and Engineering, vol.993, Article number 012111, doi:10.1088/1757-899X/993/1/012111.

[32] Shankar Goud B. (2020): *Heat Generation/Absorption influence on steady stretched permeable surface on MHD flow of a micropolar fluid through a porous medium in the presence of variable suction/injection*.– International Journal of Thermofluids, vol.7-8, Article number 100044,https://doi.org/10.1016/j.ijft.2020.100044.

[33] Shankar Goud B. (2017): *MHD flow past a vertical oscillating plate with radiation and chemical reaction in porous medium- finite difference method", International Journal of Emerging Technologies in Engineering Research*, vol.5. No.11, pp.32-35.

[34] Shankar Goud B. and Raja Shekar M.N. (2017): *Finite element study of Soret and radiation effects on mass transfer flow through a highly porous medium with heat generation and chemical reaction.*– International Journal of Computational and Applied Mathematics, vol.12, No.1, pp.53-64.

[35] Mahantesh M. Nandeppanavar M., Subhas Abel and Siddalingappa M. N. (2013*): Heat transfer through a porous medium over a stretching sheet with effect of viscous dissipation*.– Chemical Engineering Communications, vol.200, No.11, pp.1513-1529.

[36] Subhas Abel M., Siddheshwar P.G. and Nandeppanavar M.M. (2007): *Heat transfer in a viscoelastic boundary layer flow over a stretching sheet with viscous dissipation and non-uniform heat source*.– International Journal of Heat and Mass Transfer, vol.50, pp.960-966.

[37] Nandeppanavar M.M., Srinivasulu T. and Bandari S. (2020): *MHD flow and heat transfer analysis of Newtonian and non-Newtonian nanofluids due to an inclined stretching surface.*– Multidiscipline Modeling in Materials and Structures, vol.16, No.1, pp.134-155, https://doi.org/10.1108/MMMS-11-2018-0192.

[38] Subhas Abel M., Nandeppanavar M.M.and Basanagouda V. (2017): *Effects of variable viscosity, buoyancy and variable thermal conductivity on mixed convection heat transfer due to an exponentially stretching surface with magnetic field*.– Proc. Natl. Acad. Sci., India, Sect. A, Phys. Sci., vol.87, pp.247-256, https://doi.org/10.1007/s40010-016-0338-1.

Received: November 2, 2021
Revised: March 14, 2022